Computers and Mathematics with Applications 62 (2011) 725–736

Contents lists available at ScienceDirect

Computers and Mathematics with Applications

journal homepage: www.elsevier.com/locate/camwa

Double-diffusive and Soret-induced convection of a micropolar fluid in a vertical channel

Z. Alloui [a,*], H. Beji [b], P. Vasseur [a,b]

[a] Ecole Polytechnique, Université de Montréal, C.P. 6079, Succ. "Centre ville", Montréal, Québec, H3C 3A7, Canada[1]

[b] Laboratoire des Technologies Innovantes, Université Jules Vernes d'Amiens, rue des Facultés le Bailly, 800025 Amiens Cedex, France

ARTICLE INFO

Article history:
Received 24 November 2010
Received in revised form 29 May 2011
Accepted 31 May 2011

Keywords:
Natural convection
Micropolar fluid
Vertical channel
Double diffusion
Soret effect

ABSTRACT

This paper reports an investigation of the fully developed natural convection heat and mass transfer of a micropolar fluid in a vertical channel. Asymmetric temperature and concentration boundary conditions are applied to the walls of the channel. The cases of double diffusion and Soret-induced convection are both considered. The governing parameters for the problem are the buoyancy ratio and the various material parameters of the micropolar fluid. The resulting non-dimensional boundary value problem is solved analytically in closed form using MAPLE software. A numerical solution of the time dependent governing equations is demonstrated to be in good agreement with the analytical model. The influence of the governing parameters on the fluid flow as well as heat and solute transfers is demonstrated to be significant.

1. Introduction

The theory of micropolar fluids, introduced by Eringen [1–4] in order to deal with the characteristics of fluids with suspended particles, has received considerable interest in recent years. Examples of applications of such fluids include the behavior of colloidal suspensions or polymeric fluids [5], liquid crystals [6], animal blood [7], exotic lubricants [4], etc. Also, as demonstrated by Papautsky et al. [8], Eringen's model predicts successfully the characteristics of flow in microchannels. An excellent review of the various applications of micropolar fluid mechanics was presented by Ariman et al. [9,10].

The first study of the fully developed free convection of a micropolar fluid in a vertical channel was presented by Chamkha et al. [11]. This problem was extended by Kumar et al. [12] to consider the case of a channel with one region filled with micropolar fluid and the other region with a Newtonian fluid. It was found that the effects of the micropolar fluid material parameters suppress the fluid velocity but enhance the microrotation velocity. The problem of convective heat and mass transfer in a vertical channel with asymmetric wall temperatures and concentrations has been investigated by Cheng [13]. An analytical solution predicting the characteristics of fluid flow, and heat and mass transfer was derived. It was reported that an increase of the vortex viscosity parameter tends to decrease the fluid velocity in the vertical channel. The same problem was later reconsidered by Bataineh et al. [14]. An analytical solution, obtained on the basis of the homotopy analysis method, was found to be in excellent agreement with the solution of Cheng [13]. Recently, the problem of the fully developed natural convection heat and mass transfer of a micropolar fluid between porous vertical plates with asymmetric wall temperatures and concentrations was investigated by Abdulaziz and Hashim [15]. Profiles for velocity and microrotation were presented for a range of Reynolds numbers and micropolar fluid material parameters. It is demonstrated

* Corresponding author.
E-mail address: zineddine.alloui@polymtl.ca (Z. Alloui).

[1] http://www.meca.polymtl.ca/convection.

0898-1221/$ – see front matter © 2011 Elsevier Ltd. All rights reserved.
doi:10.1016/j.camwa.2011.05.053

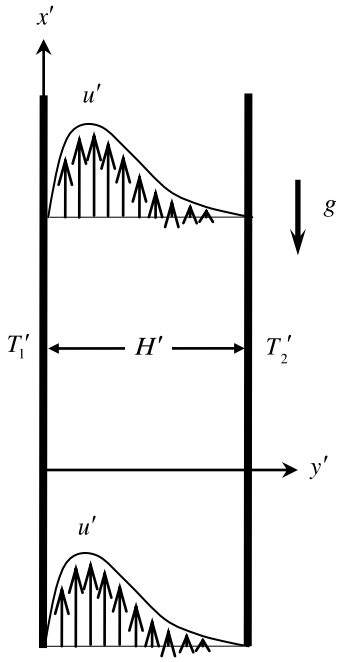

Fig. 1. The flow configuration and the coordinate system.

that, as the Reynolds number increases, the velocity decreases in the left part of the channel and increases in the right part.

The above studies [13–15] are concerned with double-diffusive convection in a vertical channel for which the flows induced by the buoyancy forces result from the imposition of both thermal and solutal boundary conditions on the vertical walls. However, it is well known that convection, in a binary mixture, can also be induced by Soret effects. For this situation the species gradients result from the imposition of a temperature gradient in an otherwise uniform-concentration mixture. In fact, convection in binary fluids can be classified into problems of two types as regards the solutal contribution to the total buoyancy force induced by the thermal and solutal gradients. In the first type of problem, called double-diffusive convection, the solutal field results from the imposition of given solutal boundary conditions on the system. In the second problem, called Soret-induced convection, the solutal gradients are due to the thermal diffusion in a binary mixture, initially homogeneous. The first study of Soret-induced convection was described by Bergman and Srinivasan [16], while considering natural convection in a cavity filled with a binary fluid. This flow configuration has also been investigated by a few authors [17–22]. As pointed out recently by Rawat and Bhargava [23], the study of heat and mass transfer in micropolar fluids is of importance in the fields of chemical engineering, aerospace engineering and also industrial manufacturing processes.

The purpose of the present paper is to extend the work of Cheng [13] by considering not only double-diffusive convection but also convection induced by the Soret effects. Furthermore, the boundary conditions considered here for the angular velocity are more general than those considered in Refs. [13–15].

2. Basic equations

We consider a steady fully developed laminar natural convection flow of a micropolar fluid between two infinite vertical plates (see Fig. 1). The vertical plates are separated by a distance H'. The convection current is induced by both the temperature and concentration gradients. The flow is assumed to be in the x' direction, which is taken to be vertically upward along the channel walls, while the y'-axis is normal to the plates. The fluid is assumed to satisfy the Boussinesq approximation, with constant properties except for the density variations in the buoyancy force term. The density variation with temperature and concentration is described by the state equation $\rho = \rho_0[1-\beta'_T(T'-T'_0)-\beta_C(C-C_0)]$ where ρ_0 is the fluid mixture density at temperature $T' = T'_0$ and mass fraction $C = C_0$, and β'_T and β_C are the thermal and the concentration expansion coefficients, respectively. In the present investigation the Dufour effect is neglected since it is well known that the modification of the heat flow due to the concentration gradient is of importance in gases but negligible in liquids. Under these assumptions, the governing equations can be written as [13]

$$(\mu+\kappa)\frac{d^2u'}{dy'^2}+\kappa\frac{dN'}{dy'} = -\rho_0 g[\beta'_T(T'-T'_0)+\beta_C(C-C_0)] \tag{1}$$

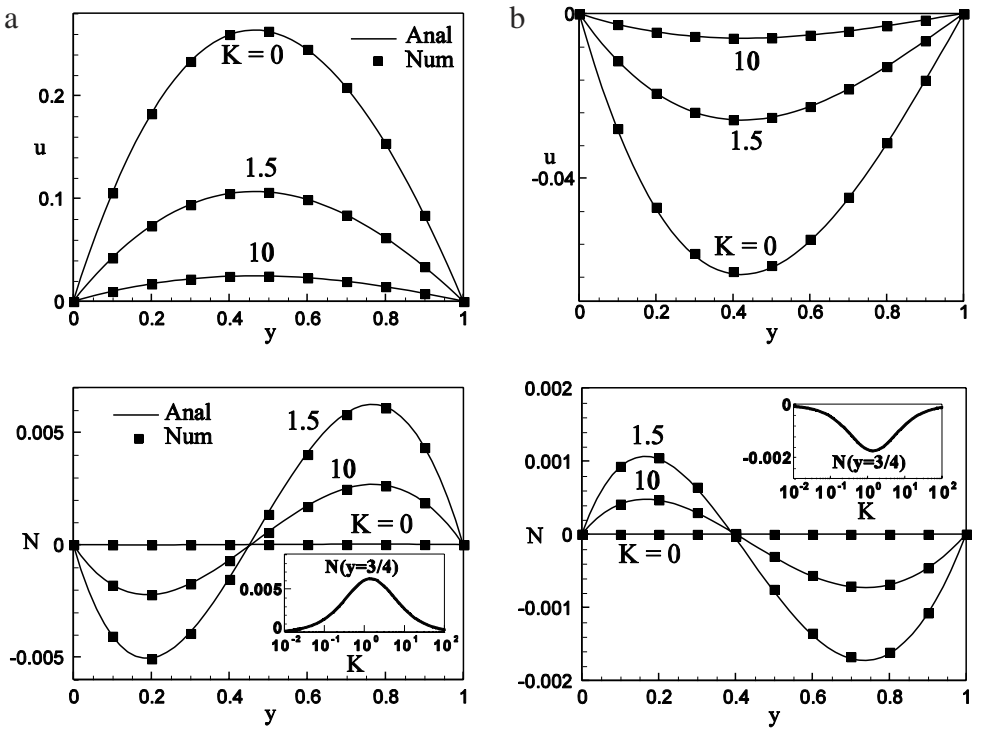

Fig. 2. Effects of parameter K on the velocity profiles u and the microrotation profiles N for $n = 0$, $a = 0$, (a) $\varphi = 2$, (b) $\varphi = -2$.

$$\frac{\gamma}{j}\frac{\mathrm{d}^2N'}{\mathrm{d}y'^2} - \frac{\kappa}{j}\left(2N' + \frac{\mathrm{d}u'}{\mathrm{d}y'}\right) = 0 \tag{2}$$

$$\frac{\mathrm{d}^2T'}{\mathrm{d}y'^2} = 0 \tag{3}$$

$$\frac{\mathrm{d}^2C}{\mathrm{d}y'^2} = 0 \tag{4}$$

where u' is the velocity component along the x' direction, and g is the acceleration due to gravity. Further, μ, κ, j, N' and γ are respectively the dynamic viscosity, vortex viscosity, micro-inertia density, angular velocity and spin gradient viscosity. Following Chamkha et al. [11] it is assumed that γ has the form $\gamma = (\mu + \kappa/2)j$.

The appropriate boundary conditions applied on the walls of the vertical channel are

$$u' = 0, \quad N' = -n\frac{\mathrm{d}u'}{\mathrm{d}y'}, \qquad T' = T'_1, \quad (1-a)C + a\frac{\mathrm{d}C}{\mathrm{d}y'} = (1-a)C_1 - a\frac{D'}{D}C_0\,(1-C_0)\,\frac{\mathrm{d}T'}{\mathrm{d}y'} \text{ on } y' = 0 \tag{5}$$

$$u' = 0, \quad N' = -n\frac{\mathrm{d}u'}{\mathrm{d}y'}, \qquad T' = T'_2, \quad (1-a)C + a\frac{\mathrm{d}C}{\mathrm{d}y'} = (1-a)C_2 - a\frac{D'}{D}C_0\,(1-C_0)\,\frac{\mathrm{d}T'}{\mathrm{d}y'} \text{ on } y' = H' \tag{6}$$

where $0 \le n \le 1$ is a boundary parameter that indicates the degree to which the microelements are free to rotate near the channel walls. The case $n = 0$ represents concentrated particle flows in which the microelements close to the wall are unable to rotate [24]. The case $n = 0.5$ represents weak concentration and corresponds to the vanishing of antisymmetric part of the stress tensor [25]. Finally, according to Peddieson [26] the case $n = 1$ is applicable to the modeling of turbulent boundary layer flows. D and D' are respectively the molecular diffusion coefficient and the thermodiffusion coefficient.

The governing equations are non-dimensionalized by scaling length by H', velocity by $\mu Gr/(\rho_0 H')$, and microrotation by $\mu Gr/(\rho_0 H'^2)$ where $Gr = g\rho_0^2\beta'_T(T_1 - T_0)H'^3/\mu^2$ is the Grashof number. Also, we introduce the reduced temperature $T = (T' - T'_0)/(T'_1 - T'_0)$ and the reduced concentration $S = (C - C_0)/\Delta C$ where $\Delta T' = T'_1 - T'_0$ and $\Delta C = C_1 - C_0$ for double-diffusive convection and $\Delta C = -C_0(1 - C_0)\Delta T' D'/D$ for Soret-driven convection. The subscript 0 indicates a reference state.

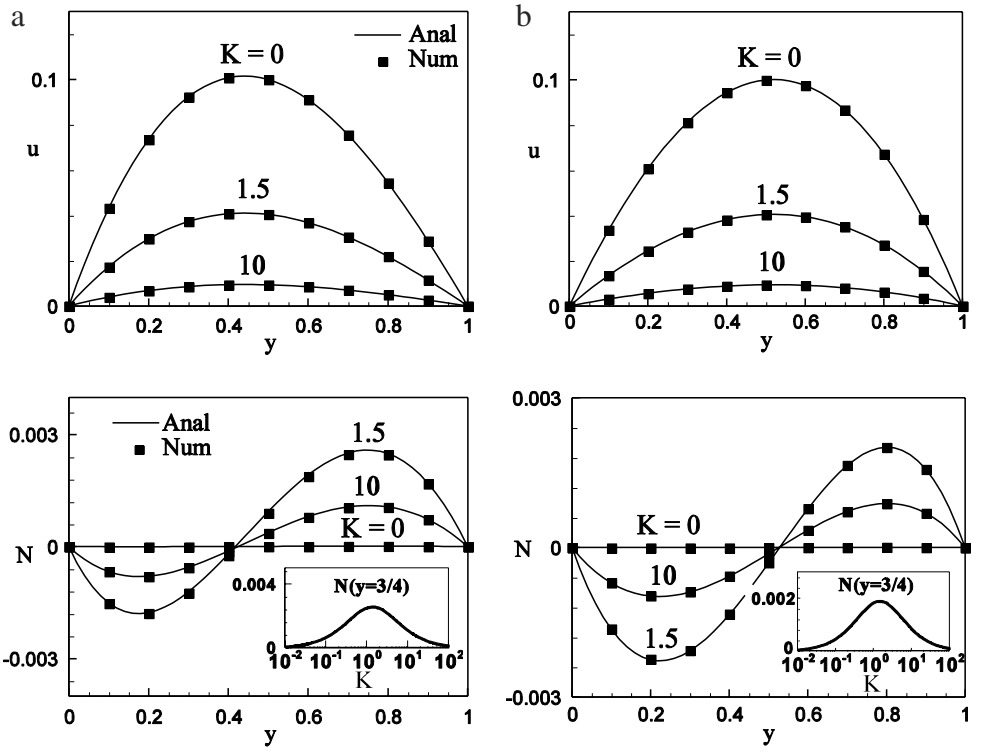

Fig. 3. Effects of parameter K on the velocity profiles u and the microrotation profiles N for $n = 0$, $a = 1$, (a) $\varphi = 2$, (b) $\varphi = -2$.

The dimensionless equations governing the present problem then read

$$(1+K)\frac{\mathrm{d}^2u}{\mathrm{d}y^2} + K\frac{\mathrm{d}N}{\mathrm{d}y} = -(T+\varphi S) \tag{7}$$

$$(1+K/2)\frac{\mathrm{d}^2N}{\mathrm{d}y^2} - BK\left(2N + \frac{\mathrm{d}u}{\mathrm{d}y}\right) = 0 \tag{8}$$

$$\frac{\mathrm{d}^2T}{\mathrm{d}y^2} = 0 \tag{9}$$

$$\frac{\mathrm{d}^2S}{\mathrm{d}y^2} = 0. \tag{10}$$

The corresponding boundary conditions in dimensionless form are

$$u = 0, \quad N = -n\frac{\mathrm{d}u}{\mathrm{d}y}, \qquad T = 1, \quad (1-a)S + a\frac{\mathrm{d}S}{\mathrm{d}y} = (1-a) + a\frac{\mathrm{d}T}{\mathrm{d}y} \text{ on } y = 0 \tag{11}$$

$$u = 0, \quad N = -n\frac{\mathrm{d}u}{\mathrm{d}y}, \qquad T = R_T, \quad (1-a)S + a\frac{\mathrm{d}S}{\mathrm{d}y} = (1-a)R_S + a\frac{\mathrm{d}T}{\mathrm{d}y} \text{ on } y = 1 \tag{12}$$

where $\varphi = \beta_C \Delta C/\beta'_T \Delta T'$ is the buoyancy ratio, $R_T = (T'_2 - T'_0)/(T'_1 - T'_0)$ is the wall temperature ratio, $R_S = (C_2 - C_0)/(C_1 - C_0)$ is the wall concentration ratio, $K = \kappa/\mu$ is the vortex viscosity parameter and $B = H'^2/j$ is the micro-inertia parameter.

In the present formulation the particular case $a = 0$ corresponds to double-diffusive convection for which the solutal buoyancy forces are induced by the imposition of a constant concentration such that $S = 1$ on $y = 0$ and $S = R_S$ on $y = 1$. On the other hand $a = 1$ corresponds to the case of a binary fluid subject to the Soret effect. For this situation, it follows from Eqs. (11) and (12) that $\mathrm{d}S/\mathrm{d}y = \mathrm{d}T/\mathrm{d}y$ on $y = 0, 1$.

3. The analytical solution

It can be shown that Eqs. (7)–(10), together with the boundary conditions Eqs. (11)–(12), possess the following analytical solution, obtained with the help of the Maple software:

$$u(y) = (C_1 \mathrm{e}^{\Omega y} + C_2 \mathrm{e}^{-\Omega y})a_5 + (a_4 - 2C_3)y - a_3 y^2 - a_2 y^3/3 + C_5 \tag{13}$$

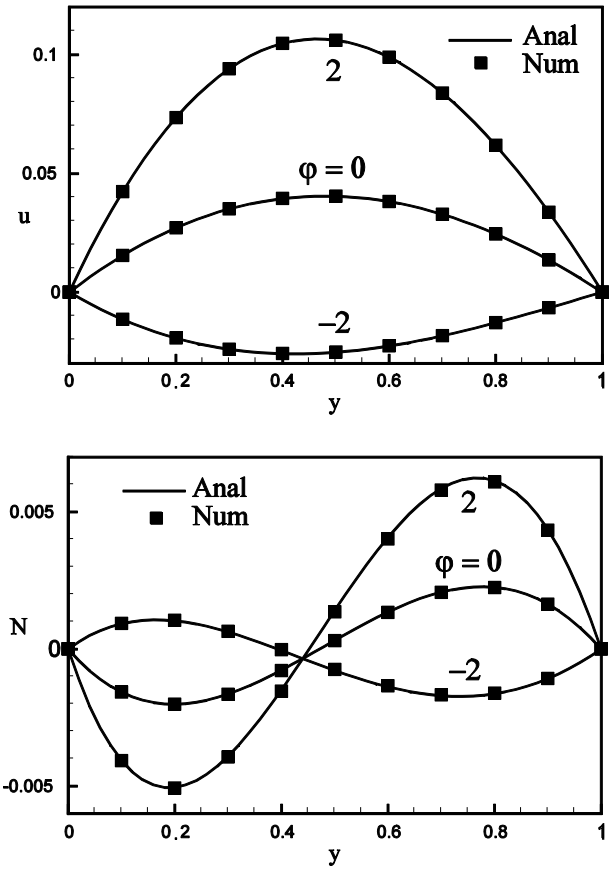

Fig. 4. Effects of buoyancy ratio φ on the velocity profiles u and the microrotation profiles N for $K = 1.5$, $n = 0$ and $a = 0$.

$$N(y) = (C_1 e^{\Omega y} - C_2 e^{-\Omega y})/\Omega + a_3 y + a_2 y^2/2 + C_3 \tag{14}$$

$$T(y) = C_4 y + 1 \tag{15}$$

$$S(y) = C_6 y + C_7 \tag{16}$$

where:

$$\begin{aligned} C_1 &= \left[2nb_1a_4 - 2b_1b_3e^{\Omega} + d_1(1 - e^{\Omega})\right]/e_1 \\ C_2 &= \left[2nb_1a_4e^{\Omega} - 2b_1b_3 + d_2(1 - e^{\Omega})\right]e^{\Omega}/e_1 \\ C_3 &= \left[b_1b_4(1 + e^{\Omega}) + d_3(1 - e^{\Omega})\right]/e_2 \\ C_4 &= R_T - 1 \\ C_5 &= \left[d_4(1 - e^{\Omega}) + d_5(1 + e^{\Omega}) - d_6e^{\Omega}\right]a_5/e_1 \\ C_6 &= (1 - a)R_S + aR_T - 1 \\ C_7 &= (1 - a) + a(1 - R_T)/2 \end{aligned} \tag{17}$$

and

$$\begin{aligned} a_1 &= (2 + K)^{-1} \\ a_2 &= a_1(\varphi C_6 + C_4) \\ a_3 &= a_1(\varphi + C_7) \\ a_4 &= a_2(1 + K/2)/(BK) \\ a_5 &= (1 + K/2)/(BK) - 2/\Omega^2 \\ b_1 &= \Omega^{-1} + na_5\Omega \\ b_2 &= 1 - 2n \\ b_3 &= (a_3 + a_2/2)b_2 + na_4 \end{aligned} \tag{18}$$

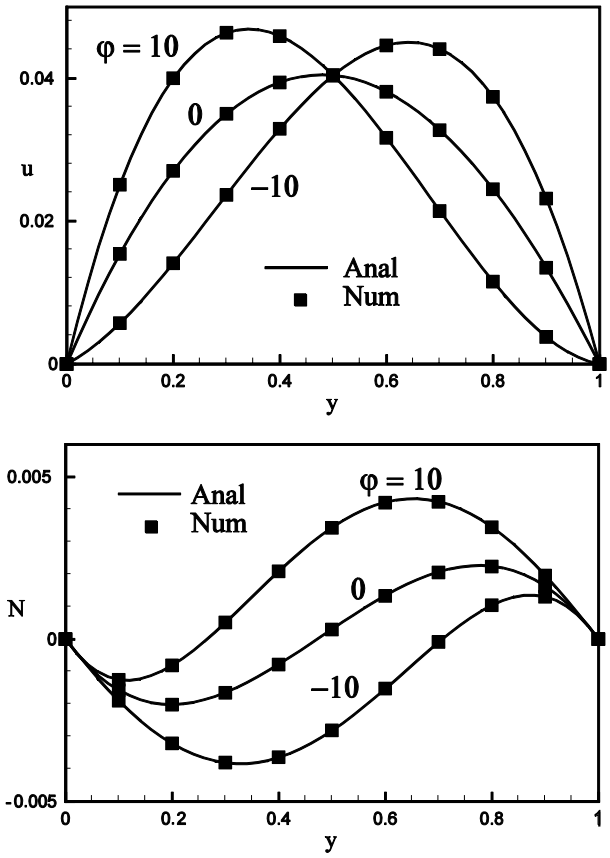

Fig. 5. Effects of buoyancy ratio φ on the velocity profiles u and the microrotation profiles N for $K = 1.5$, $n = 0$ and $a = 1$.

and

$$\begin{aligned}
d_1 &= b_1b_2b_4 + b_2b_3a_5 - nb_2a_4a_5\\
d_2 &= -b_1b_2b_4 + b_2b_3a_5 - nb_2a_4a_5\\
d_3 &= a_5b_3 + na_5a_4\\
d_4 &= b_2b_3a_5 - nb_2a_4a_5\\
d_5 &= b_1b_2b_4 + 2nb_1a_4\\
d_6 &= 2b_1b_2b_4 + 4b_1b_3\\
e_1 &= 2[b_1(1+\mathrm{e}^{\Omega}) - a_5b_2(1-\mathrm{e}^{\Omega})](\mathrm{e}^{\Omega}-1)b_1\\
e_2 &= 2[b_1(1+\mathrm{e}^{\Omega}) - a_5b_2(1-\mathrm{e}^{\Omega})]\\
\Omega^2 &= (2+K)BK/[(1+K/2)(1+K)].
\end{aligned} \tag{19}$$

The dimensionless volume flow rate is given by

$$\begin{aligned}
Q &= \int_0^1 u\mathrm{d}y\\
&= [(1-\mathrm{e}^{-\Omega})C_2 - (1-\mathrm{e}^{\Omega})C_1]a_5/\Omega + a_4/2 - C_3 - a_3/3 - a_2/12 + C_5.
\end{aligned} \tag{20}$$

The dimensionless total rates at which heat and species are added to the fluid are obtained, respectively, as follows:

$$\begin{aligned}
E &= \int_0^1 uT\mathrm{d}y\\
&= \frac{[(1-\mathrm{e}^{-\Omega})C_2 - (1-\mathrm{e}^{\Omega})C_1]a_5}{\Omega} + \frac{a_4}{2} - C_3 - \frac{a_3}{3} - \frac{a_2}{12} + C_5\\
&\quad + \left\{[(1-\mathrm{e}^{-\Omega} - \Omega\mathrm{e}^{-\Omega})C_2 - (1-\mathrm{e}^{\Omega} + \Omega\mathrm{e}^{\Omega})C_1]a_5 + \frac{a_4}{3} - \frac{2C_3}{3} - \frac{a_3}{4} - \frac{a_2}{15} + \frac{C_5}{2}\right\}C_4
\end{aligned} \tag{21}$$

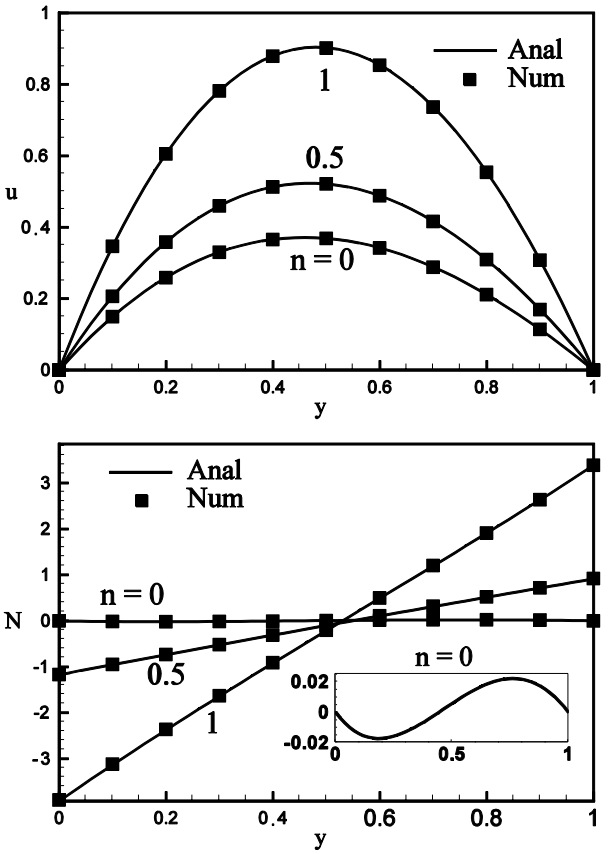

Fig. 6. Effects of parameter n on the velocity profiles u and the microrotation profiles N for $K = 1.5$, $\varphi = 10$ and $a = 0$.

$$\begin{aligned}\Phi &= \int_0^1 uS\mathrm{d}y \\ &= \left\{\frac{[(1-\mathrm{e}^{-\Omega})C_2-(1-\mathrm{e}^{\Omega})C_1]a_5}{\Omega}+\frac{a_4}{2}-C_3-\frac{a_3}{3}-\frac{a_2}{12}+C_5\right\}C_7 \\ &\quad+\left\{[(1-\mathrm{e}^{-\Omega}-\Omega\mathrm{e}^{-\Omega})C_2-(1-\mathrm{e}^{\Omega}+\Omega\mathrm{e}^{\Omega})C_1]a_5+\frac{a_4}{3}-\frac{2C_3}{3}-\frac{a_3}{4}-\frac{a_2}{15}+\frac{C_5}{2}\right\}C_6. \end{aligned} \tag{22}$$

It is noted that for the case $a = 0$ and $n = 0$, Eqs. (13)–(22) reduce to those reported by Cheng [13].

4. Results and discussion

The governing Eqs. (7)–(10), subject to boundary conditions, Eqs. (11)–(12), have been solved numerically, using an implicit finite-difference method. The unsteady state forms of these equations were discretized by using three-point central differences. The resulting sets of algebraic equations were solved by using the classical tri-diagonal Thomas algorithm. Constant time steps of 0.01 were used while the computational domain was divided into 40 points. This mesh size was found to be sufficiently accurate, as illustrated in Table 1 for the case $K = 1.5$, $\varphi = 2$, $R_T = 0.6$, $R_S = 0.3$, $n = 0$ and for $a = 0$. The results indicate that even for a mesh size of 10 the numerical data are quite close to those predicted by the present analytical model. Thus, the computational domain was divided into 40 points for all the numerical results presented here. In view of the numerous parameters involved in the present problem the micro-inertia parameter, B, is fixed equal to 1. Also, for comparison with the results reported in Refs. [13,14], the wall temperature ratio and wall concentration ratio are maintained constant at $R_T = 0.6$ and $R_S = 0.3$. The effects of the other governing parameters, namely the buoyancy ratio φ, vortex viscosity parameter K, dimensionless micro-gyration n and constant a are illustrated in Figs. 2–9. In general it is observed that the agreement between the analytical and the numerical solutions is excellent. All the numerical results reported in this study indicate that the solution is steady in the range of the governing parameters considered here.

Figs. 2 and 3 illustrate the influence of the vortex viscosity parameter K on the distribution of velocity u and angular velocity N for $n = 0$, $a = 0$ and $a = 1$. Figs. 2(a) and 3(a) show the results obtained for $\varphi = 2$, for which the thermal and solutal buoyancy forces are cooperating. In general K depends on the shape and concentration of the microelements. For a

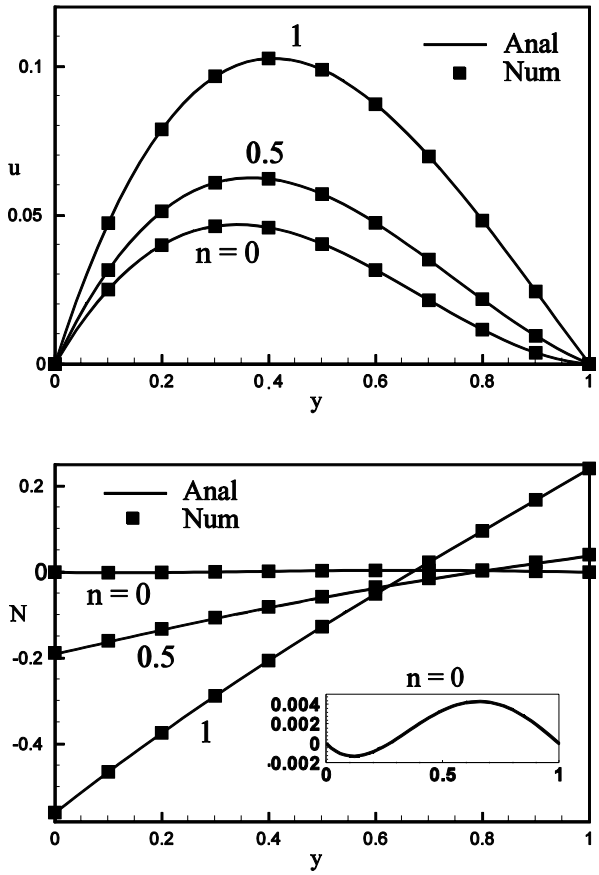

Fig. 7. Effects of parameter n on the velocity profiles u and the microrotation profiles N for $K = 1.5$, $\varphi = 10$ and $a = 1$.

Table 1
Comparison between the numerical and analytical solutions for $K = 1.5$, $B = 1$, $\varphi = 2$, $R_T = 0.6$, $R_S = 0.3$, $n = 0$ and $a = 0$.

Numerical							Analytical
Grid	10	20	40	80	160	320	
$u\left(\frac{1}{2}\right) \times 10$	1.06046	1.06081	1.06089	1.06092	1.06092	1.06092	1.06092
$N\left(\frac{1}{2}\right) \times 10^2$	0.13497	0.13930	0.14039	0.14066	0.14073	0.14075	0.14075

given shape of the microelements, K directly gives a measure of concentration of the microelements. Thus, an increase of K, i.e. of the concentration of microconstituents, results in a larger resistance to the fluid motion. Consequently, it is observed from Figs. 2 and 3 that, upon increasing parameter K, the intensity of the convective velocity u is reduced as compared to the Newtonian fluid situation ($K = 0$). In fact, according to the present theory, it is found that $u \to 0$ as the vortex viscosity parameter $K \to \infty$. In general, a review of the literature indicates that $0 \leq K \leq 10$. In Fig. 2 this range has been extended to illustrate the effect of $K \to \infty$ on N. The influence of parameter K on the angular velocity N is also illustrated in these graphs. Naturally, $N = 0$ for $K = 0$, since no rotation can occur in the absence of micropolar elements (Newtonian fluid situation). The variation with K of the value of N, evaluated at the position $y = 3/4$, is also presented in the graphs. The results indicate that upon increasing K the intensity of N first increases. However, for K above unity, the value of N starts to decrease. The fact that a critical value of the viscosity ratio exists for N has already been reported in the past by Kim and Kim [27], while studying plane Couette micropolar flows. For this geometry it was demonstrated that the critical value of N occurs at about $K = 0.3$. The same phenomenon was also reported by Alloui and Vasseur [28] for the case of a layer of micropolar fluid heated from the bottom by a constant heat flux. A bird's eye view of the results presented in these graphs indicates that the flow characteristics, obtained for double-diffusive convection and Soret-induced convection, are qualitatively similar. However, it is clear that the strength of the convection is higher for the double-diffusive situation. Figs. 2(b) and 3(b) show the results obtained for $\varphi = -2$, i.e. when thermal and solutal buoyancy forces are opposing each other. For this situation, in the case of double-diffusive convection, Fig. 2(b) indicates that the flow direction is now downward, since the solutal buoyancy forces are predominant. This is not the case for Soret-induced convection where, as can be observed from Fig. 3(b), the flow remains upward. For this situation, a higher negative value of φ is required to obtain

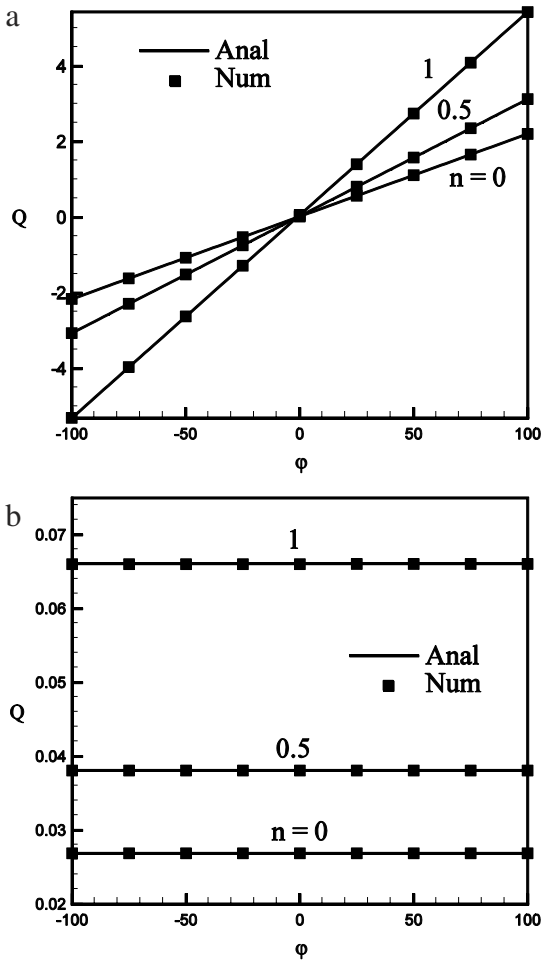

Fig. 8. Effects of buoyancy ratio φ and parameter n on the volume flow rate Q for $K = 1.5$, (a) $a = 0$, (b) $a = 1$.

a downward flow. As can be observed from Figs. 4 and 5 the influence of φ on u and N is considerably more important in double-diffusive convection than in Soret-induced convection.

The effect of the buoyancy ratio φ on the velocity profiles u and microrotation profiles N is exemplified in Figs. 4 and 5 for the cases $a = 0$ and $a = 1$, respectively. In the absence of solute concentration effects, i.e. when $\varphi = 0$, the flow is induced solely by the imposed temperature gradients. The graphs show that for this situation, as expected, both the intensity of convection u and the microrotation N are the same independently of the convective mode (double diffusion or Soret-induced convection). In the case of double diffusion, Fig. 4 indicates that, when φ is above zero, the thermal and solutal buoyancy forces act in the same direction and the flow is considered to be aided. Thus for $\varphi = 2$, it is found that the magnitudes of the fluid velocity and the microrotation are promoted in the vertical channel. On the other hand, when φ is below zero the thermal and solutal buoyancy forces act now in opposing directions. As a result, for $\varphi = -2$, the flow direction is now reversed since it is governed by the predominant solutal effects. Naturally, the same trend is observed for the microrotation profiles. On the other hand, in the case of Soret-induced convection, Fig. 5 shows that the trend is quite different. Thus upon increasing (decreasing) φ from zero to 10 (-10) it is seen that the strength of convection is enhanced, the peak velocity being moving toward the left (right) hotter (colder) wall. As discussed below, upon increasing φ considerably the flow pattern is, depending on the sign of this parameter, up or down in the halves of the channel.

The influence of micro-gyration parameter n on the velocity u, and microrotation N profiles, for $K = 1.5$ and $\varphi = 10$, is depicted in Fig. 6 for $a = 0$ and Fig. 7 for $a = 1$. The results indicate that the intensity of the convective flow u and that of the angular velocity N are minimum for $n = 0$. This particular value of n represents the case where the concentration of the microelements is sufficiently large that the particles close to the walls are unable to rotate. Upon increasing the value of n, the concentration of the solution becomes weaker such that the particles near the walls are free to rotate. Thus, as n is augmented the microrotation term is augmented, which induces an enhancement of the flow.

Fig. 8(a) and (b) show the variation of the dimensionless flow rate, Q, with the buoyancy ratio φ for $K = 1.5$ and various values of the micro-gyration parameter n. For the case of double-diffusive convection it is observed that when both the

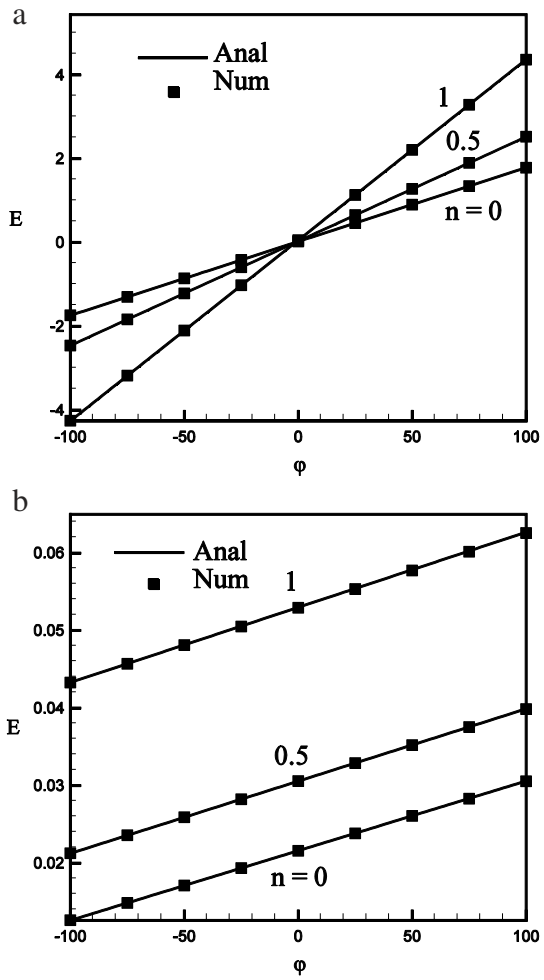

Fig. 9. Effects of buoyancy ratio φ and parameter n on the total rate at which heat is added to the fluid, E, for $K = 1.5$, (a) $a = 0$, (b) $a = 1$.

thermal and solutal buoyancy forces are aiding ($\varphi > 0$), the flow direction is upward ($Q > 0$). The reverse is true ($Q < 0$) when both the thermal and solutal buoyancy forces are opposing ($\varphi < 0$). On the other hand, for the case of Soret-induced convection, the flow rate is found to be independent of the buoyancy ratio φ. This follows from the fact that, for this situation, the quantity of the solute between the two vertical plates remains constant. The Soret effect acts merely to redistribute the concentration in the system, giving rise to local increase or decrease of the local velocity. However, the global flow rate remains constant. Also, as discussed above, upon increasing the value of n the intensity of the velocity field (and thus of the flow rate Q) is enhanced.

The dimensionless total rate, E, at which heat is added to the fluid is plotted in Fig. 9(a) and (b) as a function of the buoyancy ratio φ and the micro-gyration parameter n, for the case $K = 1.5$. Fig. 9(a) shows that, in the case of double-diffusive convection, for $\varphi > 0$, increasing φ results in an augmentation of the strength of the convective motion such that E increases. For $\varphi < 0$, the results are similar but, since the flow direction is now downward, the value of E is negative. On the other hand the results obtained for Soret-induced convection, Fig. 9(b), are quite different. For this situation, the velocity profiles (not presented here) indicate that for $\varphi \gg 1$ the flow is upward near the left hotter wall and downward near the right colder one. Thus, the total rate E at which heat is added to the fluid is promoted upon increasing φ as a result of the increase of the flow intensity near the hotter wall. Naturally, for large negative values of φ the flow direction is reversed (downward near the hot wall and upward near the cold wall). Thus, the value of E decreases and becomes eventually negative (for instance, this happens at $\varphi \leq -240$ when $n = 0$). Finally, Fig. 9(a) and (b) indicate that increasing n promotes the fluid flow and thus the total rate at which heat is added to the fluid.

We now consider the buoyancy ratio. The dimensionless total rate, Φ, at which species are added to the fluid is depicted in Fig. 10 as a function of φ and the micro-gyration parameter n, for the case $K = 1.5$. The Soret-induced convection, represented by a dotted line, indicates that $\Phi = 0$ independently of n. This is expected since for this situation the solid boundaries are impermeable to concentration. The Soret effect is merely to redistribute the originally uniform concentration within the system. However, for double diffusion, the solid lines indicate that increasing φ, i.e. increasing the strength of

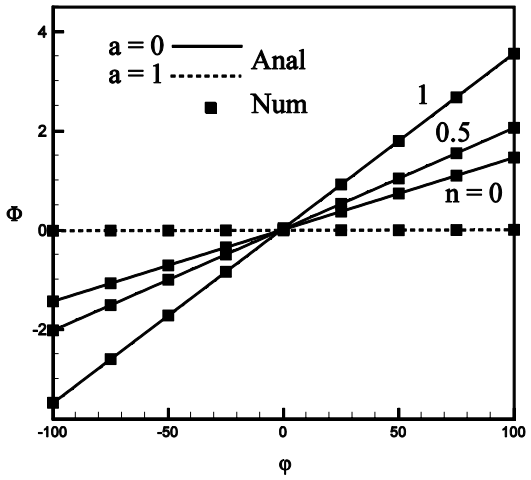

Fig. 10. Effects of buoyancy ratio φ and parameter n on the total rate at which species are added to the fluid, Φ, for $K = 1.5$, $a = 0$ and $a = 1$.

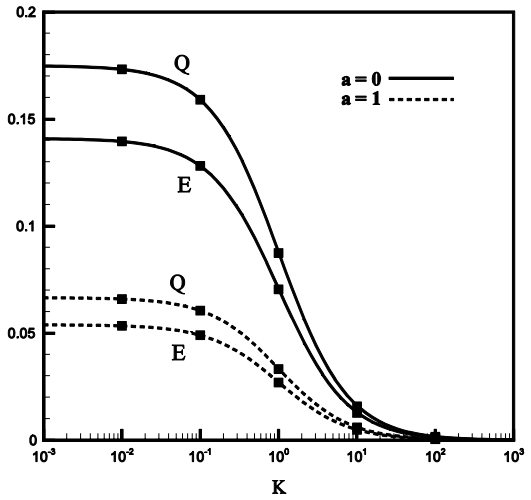

Fig. 11. Effects of parameter K on the volume flow rate Q and on the total rate at which heat is added to the fluid for $\varphi = 2$ and $n = 0$.

the convective flow, results in an enhancement of the rate of mass transfer through the system. These results are similar to those reported by Cheng [13]. Also, it is observed from Fig. 10 that, for a given value of φ, Φ decreases as the value of n is reduced toward $n = 0$. As already mentioned, a decrease of n corresponds to an increase of the concentration of the solution such that the particles close to the solid boundaries are unable to rotate. This results in a decrease of the flow rate and thus a decrease of Φ.

The volume flow rate, Q, and total rate at which heat is added to the fluid, E, are plotted in Fig. 11 as a function of K for $\varphi = 2$ and $n = 0$. Here again, the results obtained for double-diffusive convection and Soret-induced convection are qualitatively similar. In the limit $K \to 0$ both Q and E tend asymptotically to constant values corresponding to the Newtonian fluid situation. On the other hand, in the limit $K \to \infty$, both Q and E become negligible, due to the increase of the vortex viscosity.

5. Conclusions

In this paper we have studied free convection of heat and mass transfer of micropolar fluid in a vertical channel. The cases of double-diffusive convection and Soret-induced convection are both investigated. Asymmetric wall temperatures and concentrations are considered. The closed form solution proposed in this paper, for fully developed flow, is found to be in excellent agreement with a numerical solution of the time dependent form of the governing equations. Thus, in the range of the governing parameters considered in this study, the solution is steady. In general it is found that, upon increasing the vortex viscosity parameter K, the fluid velocity is inhibited. The influence of micro-gyration parameter n, which characterizes the boundary conditions applied on rotation of the microelements near the solid boundaries, on the velocity u and microrotation N profiles is found to be significant. Thus, as n is augmented, the microrotation term is

promoted, which induces enhancement of flow velocities. The effect of the buoyancy ratio φ on the velocity profiles u and microrotation profiles N is also found to be important. The flow direction in the channel depends strongly on the sign of this parameter. The results presented in this paper illustrate the difference between double diffusion [13] and Soret-induced convection. For instance the rate of flow Q within the channel is found to be independent of the buoyancy ratio φ. This is not the case for double-diffusive convection where Q is observed to depend considerably upon φ. Also the results indicate that, for given values of φ and n, the influence of K on u and N is higher for $a = 0$ than $a = 1$. A similar trend is observed for the effect of φ on u and N, for fixed values of K and n. The total rate at which heat is added to the fluid is found to be considerably higher for double diffusion than Soret convection. Finally, it is must be mentioned that in the case of $a = 0$ and $n = 0$ the present results are similar to those reported by Chen [13]. As regards the Soret-induced convection, this flow configuration does not seem, to the authors' knowledge, to have been investigated in the past.

References

[1] A.C. Eringen, Nonlinear theory of simple micro-elastic solids, Internat. J. Engrg. Sci. 2 (1964) 189–203.
[2] A.C. Eringen, Theory of micropolar fluids, J. Appl. Math. Mech. 16 (1966) 1–18.
[3] A.C. Eringen, Non-Local Polar Field Theory, Academic Press, New York, 1976.
[4] A.C. Eringen, Theory of thermomicrofluids, J. Math. Anal. Appl. 38 (1972) 480–496.
[5] B. Hudimoto, T. Tokuoka, Two-dimensional shear flows of linear micropolar fluids, Internat. J. Engrg. Sci. 7 (1969) 515–522.
[6] F. Lockwood, F. Benchaita, S. Friberg, Study of lyotropic liquid crystals in viscometric flow and elastohydrodynamic contact, Tribol. Trans., ASLE 30 (1987) 539–548.
[7] T. Ariman, M.A. Turk, N.D. Sylvester, On steady and pulsatile flow of blood, J. Appl. Math. 41 (1974) 1–7.
[8] I. Papautsky, J. Brazzle, T. Ameel, A.B. Frazier, Laminar fluid behavior in microchannels using micropolar fluid theory, Sensors Actuators 73 (1999) 101–108.
[9] T. Ariman, M.A. Turk, N.D. Sylvester, Microcontinuum fluid mechanics—a review, Int. J. Sci. 11 (1973) 905–930.
[10] T. Ariman, M.A. Turk, N.D. Sylvester, Applications to microcontinuum fluid mechanics—a review, Int. J. Sci. 12 (1974) 273–293.
[11] A.J. Chamkha, T. Grosan, I. Pop, Fully developed free convection of a micropolar fluid in a vertical channel, Int. Commun. Heat Mass Transfer 29 (2002) 1119–1127.
[12] J.P. Kumar, J.C. Umavathi, Ali J. Chamkha, I. Pop, Fully-developed free-convection of micropolar and viscous fluids in a vertical channel, Appl. Math. Model. 34 (2010) 1175–1186.
[13] C.Y. Cheng, Fully developed natural convection heat and mass transfer of a micropolar fluid in a vertical channel with asymmetric wall temperatures and concentrations, Int. Commun. Heat Mass Transfer 33 (2006) 627–635.
[14] A.S. Bataineh, M.S.M. Noorani, I. Hashim, Solutions of fully developed free convection of micropolar fluid in a vertical channel by homotopy analysis method, Internat. J. Numer. Methods Fluids 60 (2009) 779–789.
[15] O. Abdulaziz, I. Hashim, Fully developed free convection heat mass transfer of a micropolar fluid between porous vertical plates, Numer. Heat Transfer, Part A Appl. 55 (2009) 270–288.
[16] T.L. Bergman, R. Srinivasan, Numerical simulation of Soret-induced double diffusion in an initially uniform concentration binary fluid, Int. J. Heat Mass Transfer 32 (1989) 679–687.
[17] P. Traore, A. Mojtabi, Analyse de l'effet Soret en convection thermosolutale, Entropie 184 (185) (1989) 32–37.
[18] R. Krishnan, A numerical study of the instability of double-diffusive convection in a square enclosure with horizontal temperature and concentration gradients, heat transfer in convective flows, in: HTD ASME National Heat Transfer Conference, Philadelphia, vol. 107, 1989, pp. 357–368.
[19] D. Gobin, R. Bennacer, Double-diffusion convection in a vertical fluid layer: onset of the convection regime, Phys. Fluids 6 (1994) 59–67.
[20] S.R. De Groot, P. Mazur, Non Equilibrium Thermodynamics, North Holland, 1969.
[21] M. Ouriemi, P. Vasseur, A. Bahloul, L. Robillard, Natural convection in a horizontal layer of a binary mixture, Int. J. Therm. Sci. 45 (2006) 752–759.
[22] M. Ouriemi, P. Vasseur, A. Bahloul, Natural convection in inclined enclosures filled with a binary mixture, Numer. Heat Transfer 48 (2005) 547–567.
[23] S. Rawat, R. Bhargava, Finite element study of natural convection heat and mass transfer in a micropolar fluid-saturated porous regime with Soret/Dufour effect, Int. J. Appl. Math. Mech. 5 (2009) 58–71.
[24] S.K. Jena, M.N. Mathur, Similarity solutions for laminar free convection flow of a thermomicropolar fluid past a nonisothermal vertical plate, Internat. J. Engrg. Sci. 19 (1981) 1431–1439.
[25] G. Ahmadi, Self-similar solutions of incompressible micropolar boundary layer flow over a semi-infinite plate, Internat. J. Engrg. Sci. 14 (1976) 639–646.
[26] J. Peddieson, An application of the micropolar fluid model to the calculation of a turbulent shear flow, Internat. J. Engrg. Sci. 10 (1972) 23–32.
[27] Y.J. Kim, T.A. Kim, A study on the plane Couette flow using micropolar fluid theory, J. Mech. Sci. Technol. 18 (3) (2004) 491–498.
[28] Z. Alloui, P. Vasseur, Natural convection in a shallow cavity filled with a micropolar fluid, Int. J. Heat Mass Transfer 53 (2010) 2750–2759.